**Electronic Supporting Information (ESI)**

# Efficient degradation of azo dyes using Ag and Au nanoparticles stabilized on graphene oxide functionalized with PAMAM dendrimer

**Rajendiran Rajesh[a], S. Senthil Kumar[b] and Rengarajan Venkatesan[a*]**

*[a]Department of Chemistry, Pondicherry University, Puducherry-605014, India.*
*Corresponding authors: Fax; +91-413-2655987;Tel:+91-413-2654415;*
*E-mail: venkatesanr.che@pondiuni.edu.in (R.Venkatesan)*

*[b]Environmental & Analytical Chemistry Division, School of Advanced Sciences, VIT University, Vellore-632014, India.*

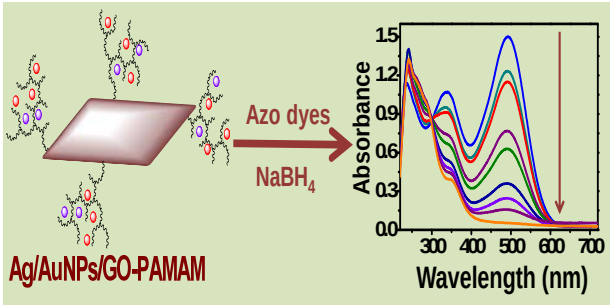

**Contents** **Page No**

**Results and discussions**

## Results and discussion

### 1.1 Thermal gravimetry analysis (TGA)

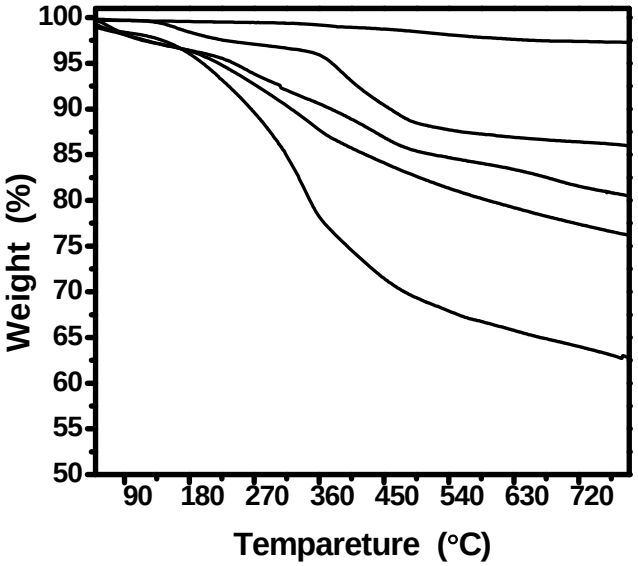


**Fig. S1.** TGA thermograms of (a) pure graphite, (b) GO, (c) GO-G1PAMAM, (d) GO-G2PAMAM and (e) GO-G3PAMAM dendrimer.

The grafted content of the PAMAM dendrimer-modified GO can be calculated from the weight loss between 200 ºC and 800 ºC.[1,2] TGA results Fig. S1 demonstrates no weight loss for pure graphite. However, the graphene oxide shows weight loss ~11% between 100 ºC-150 ºC due to pyrolysis of -OH and -COOH groups.[3-6] In the case of PAMAM dendrimers grafted GO additional weight losses from organic moieties were also seen and the weight losses were estimated as 16%, 20%, 34%, for GO-G1PAMAM, GO-G2PAMAM, GO-G3PAMAM in the temperature range 200-800 ºC. The gradual increase in weight loss from G1PAMAM to G3PAMAM indicates expansion of PAMAM dendrimer network.

### 1.2 FT-IR spectroscopy (FT-IR)

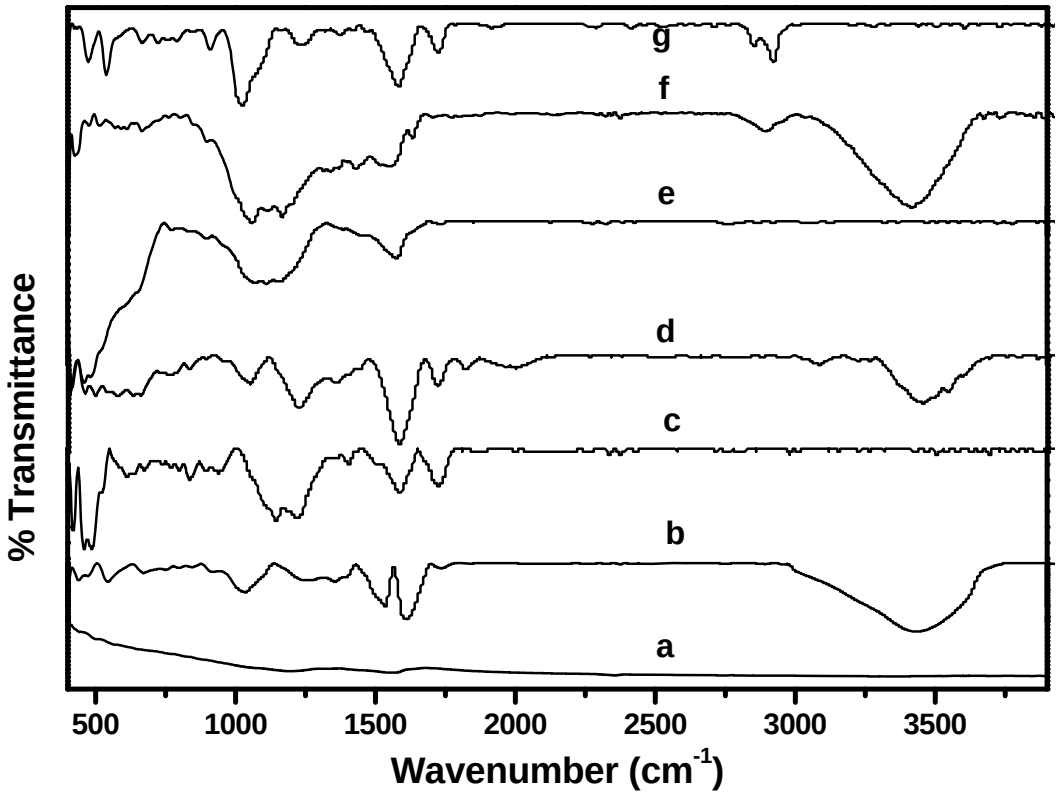


**Fig. S2.** FT-IR Spectra of (a) pure graphite, (b) GO, (c) GO-COCl, (d) GO-$CONH_2$, (e) GO-Methacrylate, (f) GO-G1PAMAM dendrimer, (g) AgNPs/GO-G1PAMAM.

Further evidence of PAMAM dendrimer exfoliation on the GO surface is provided by the infrared spectroscopy. The FT-IR spectra of pure Graphite (Fig. S2 a) shows the stretching vibrations of 1650 and 1380 $cm^{-1}$ whose origins are due to the stretching vibration of C=C and C-C groups respectively.[7,8] In the case of GO (Fig. S2 b) broad and intense peaks at 3436, 1734, and 1258 $cm^{-1}$ are newly observed and these peaks are due to the characteristic stretching vibration of O–H, C=O, and C–O group, respectively. The acylated GO (GO-COCl) (Fig. 2c) shows complete disappearance of 3436 $cm^{-1}$ peak and a new peak at 694 $cm^{-1}$ along with a shift in C=O peak shifted to 1694 $cm^{-1}$ confirming C–Cl bond formation. The addition of ethylenediamine (Fig. S2 d) on to the GO surface was confirmed through the appearance of amide band, -CONH-, at 1645 $cm^{-1}$ and -$NH_2$ group appearing at 3435 $cm^{-1}$.

The formation of GO-Methylacrylate (Fig. S2 e) was ensured through the vanishing of 3435 $cm^{-1}$ signal and appearance of ester peak at 1670 $cm^{-1}$. The confirmation of GO-G1PAMAM dendrimer (Fig. S2 f) could be seen through appearance of -$NH_2$ peak at 3435 $cm^{-1}$ and C=O peak at 1722 $cm^{-1}$.[9] Other PAMAM dendrimer grafted samples exhibited similar behavior. The disapearance of peaks corresponding to -$NH_2$ and -OH functionalities in the range between 3000 to 3500 $cm^{-1}$ in (Fig. S2 g) shows that the metal nanoparticles are stabilised in the PAMAM dendritic network through these functional groups.

### 1.3 Scanning Electron Microscope (SEM)

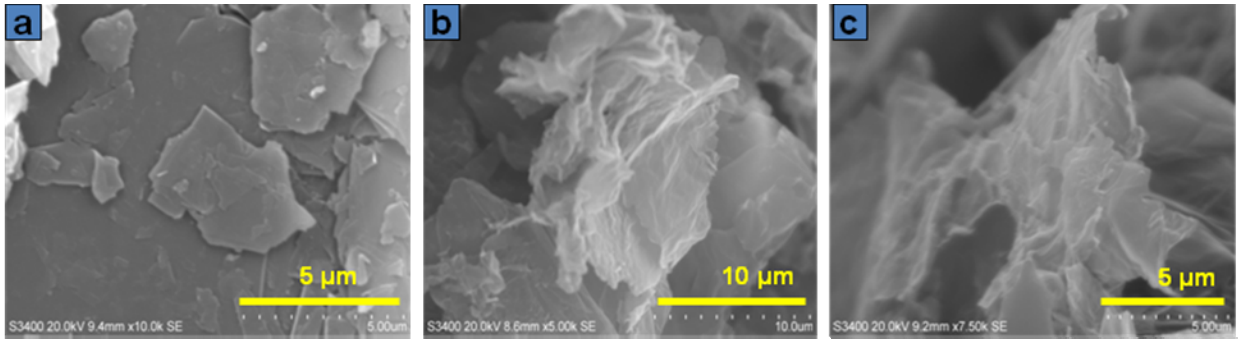


**Fig. S3** SEM images of (a) pure graphite, (b, c) GO-G3PAMAM

## 1.4 High Resolution Transmission Electron Microscopy (HR-TEM)

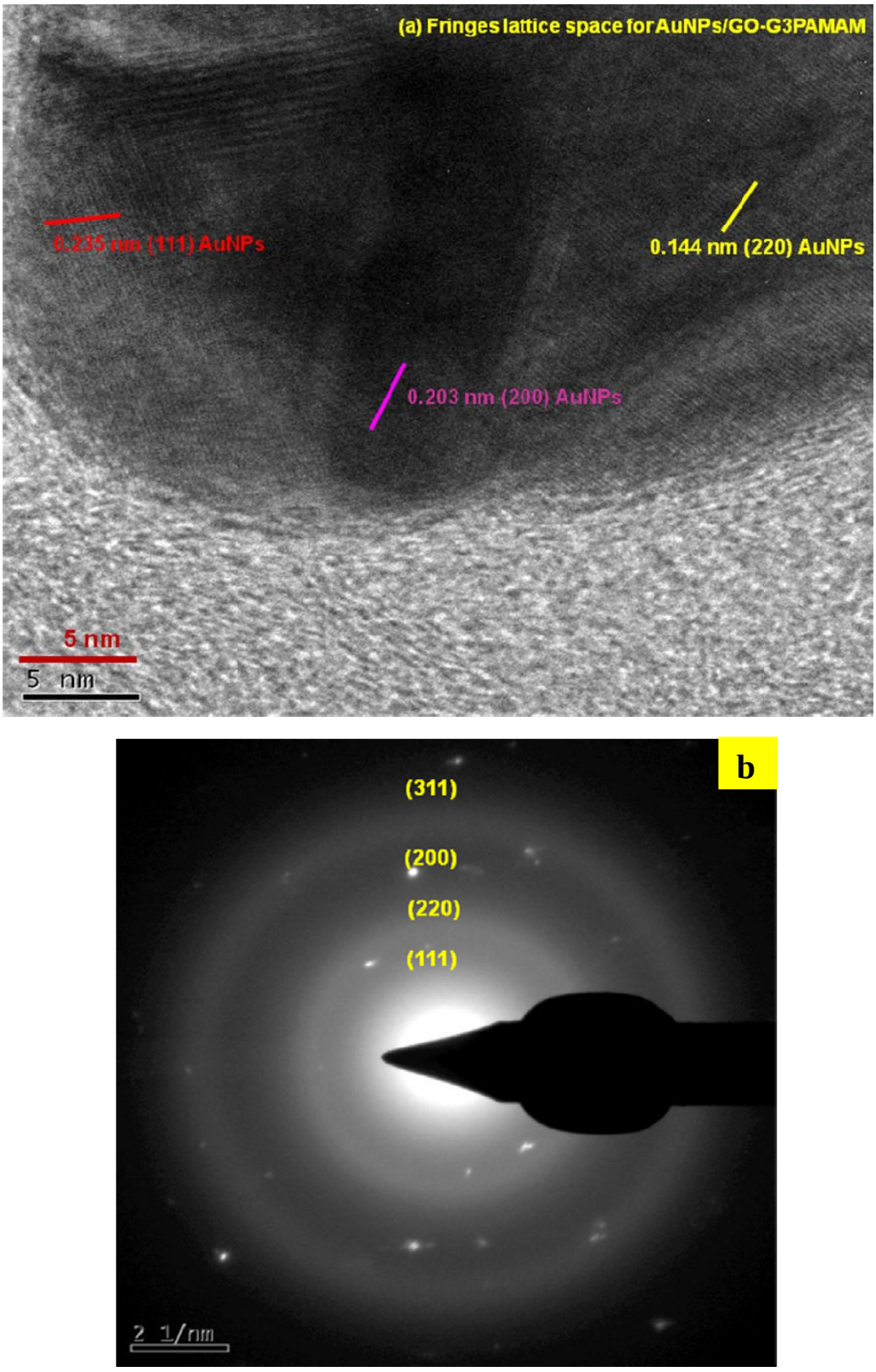


**Fig. S4** TEM images of (a, b) AuNPs/GO-G3PAMAM

## 2. Degradation of methy orange and congo red

### Degradation of organic azo dyes using Ag/AuNPs-GO-G1,2,3PAMAM

Degradation of methyl orange by AgNPs/GO-G1,2,3PAMAM dendrimer in presence of $NaBH_4$.

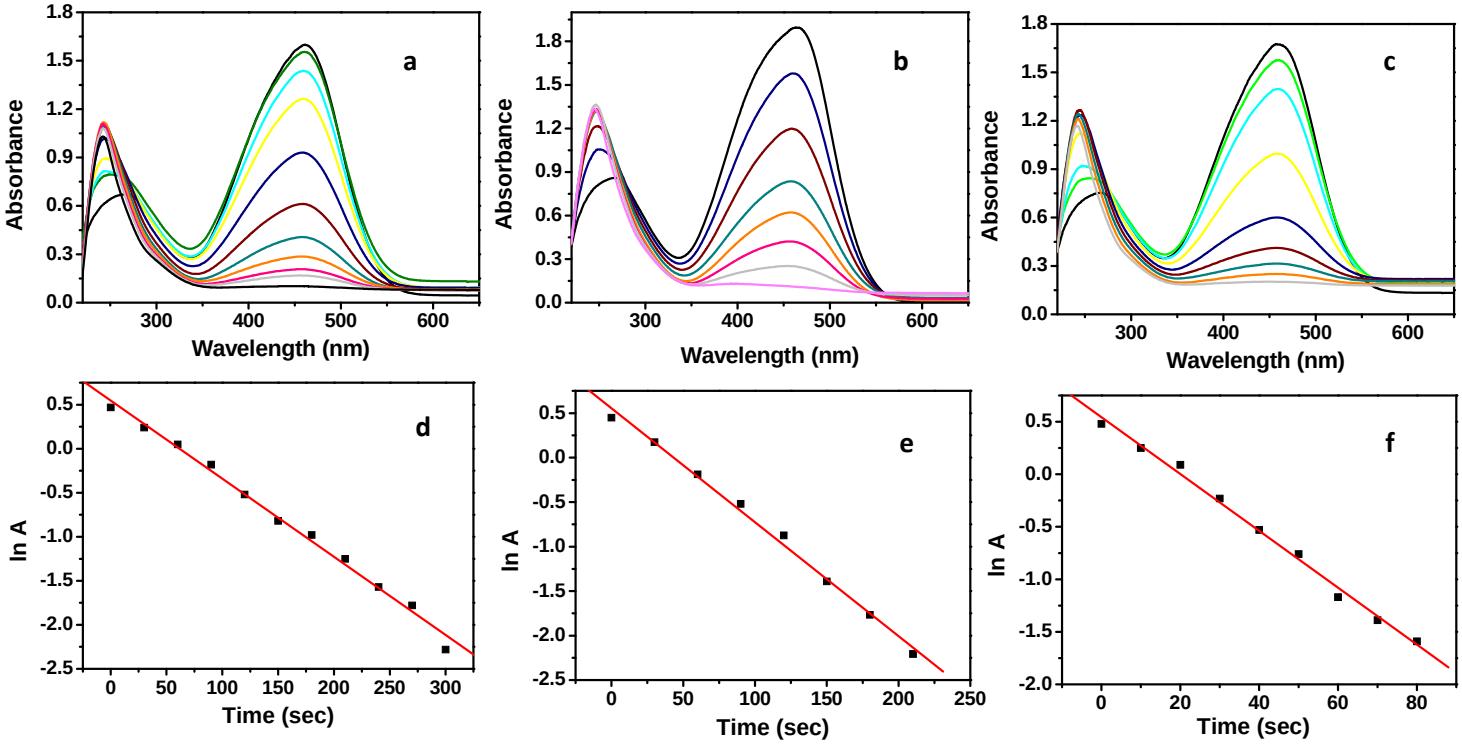


**Fig. S5** UV-Vis kinetic spectra for the degradation of methyl orange measured in varies time intervals using (a, b, c) AgNPs/GO-G1,2,3PAMAM dendrimer respectively. ln A vs Time plot for degradation of methyl orange by (d, e, f) AgNPs/GO-G1,2,3PAMAM dendrimer respectivley.

Degradation of congo red by AgNPs/GO-G1,2,3PAMAM dendrimer in presence of $NaBH_4$

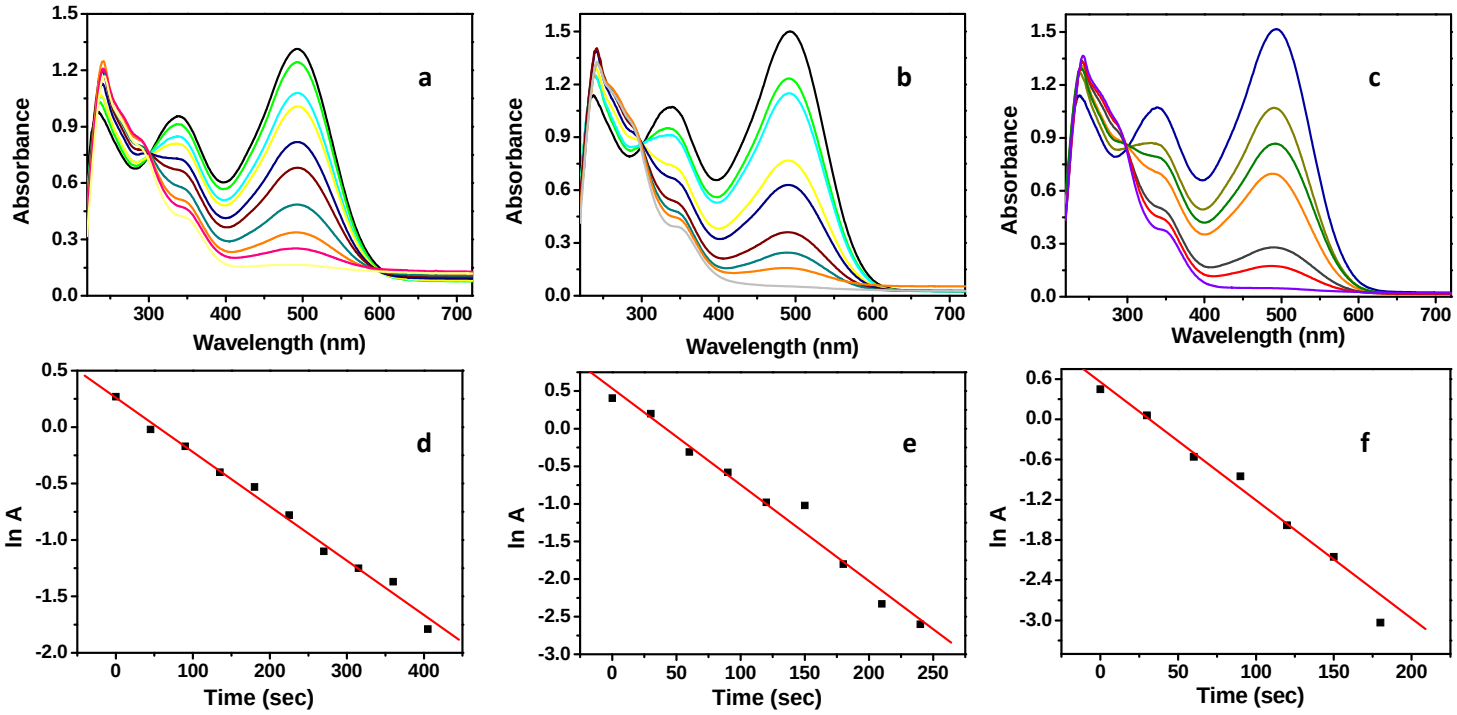


**Fig. S6** UV-Vis kinetic spectra for the degradation of congo red measured in varies time intervals using (a, b, c) AgNPs/GO-G1,2,3PAMAM dendrimer respectively. ln A vs Time plot for degradation of congo red by (d, e, f) AgNPs/GO-G1,2,3PAMAM dendrimer respectivley.

Degradation of methyl orange by AuNPs/GO-G1,2,3PAMAM dendrimer in presence of $NaBH_4$

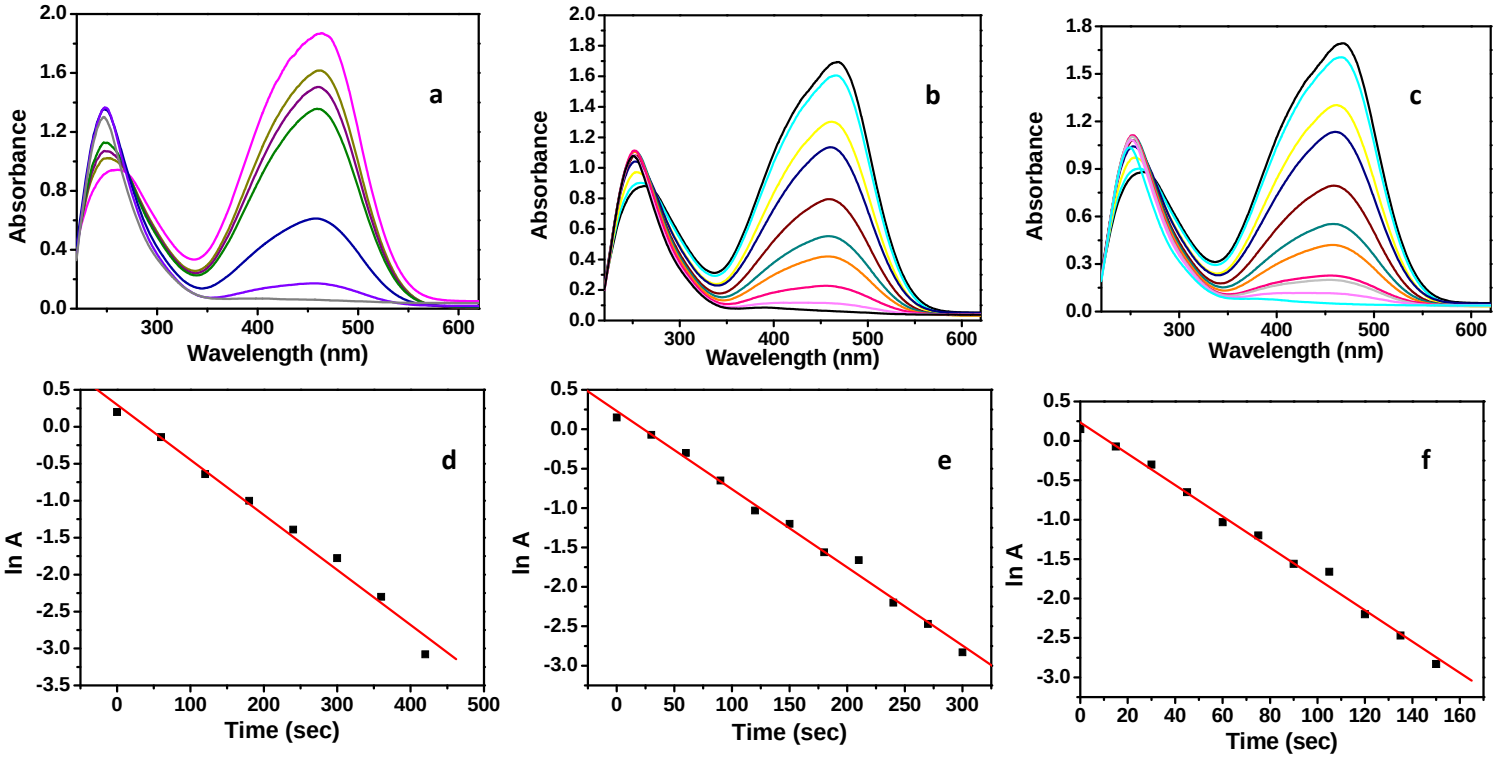


**Fig. S7** UV-Vis kinetic spectra for the degradation of methyl orange measured in varies time intervals using (a, b, c) AuNPs/GO-G1,2,3PAMAM dendrimer respectively. ln A vs Time plot for degradation of methyl orange by (d, e, f) AuNPs/GO-G1,2,3PAMAM dendrimer respectivley.

Degradation of congo red by AuNPs/GO-G1,2,3PAMAM dendrimer in presence of $NaBH_4$

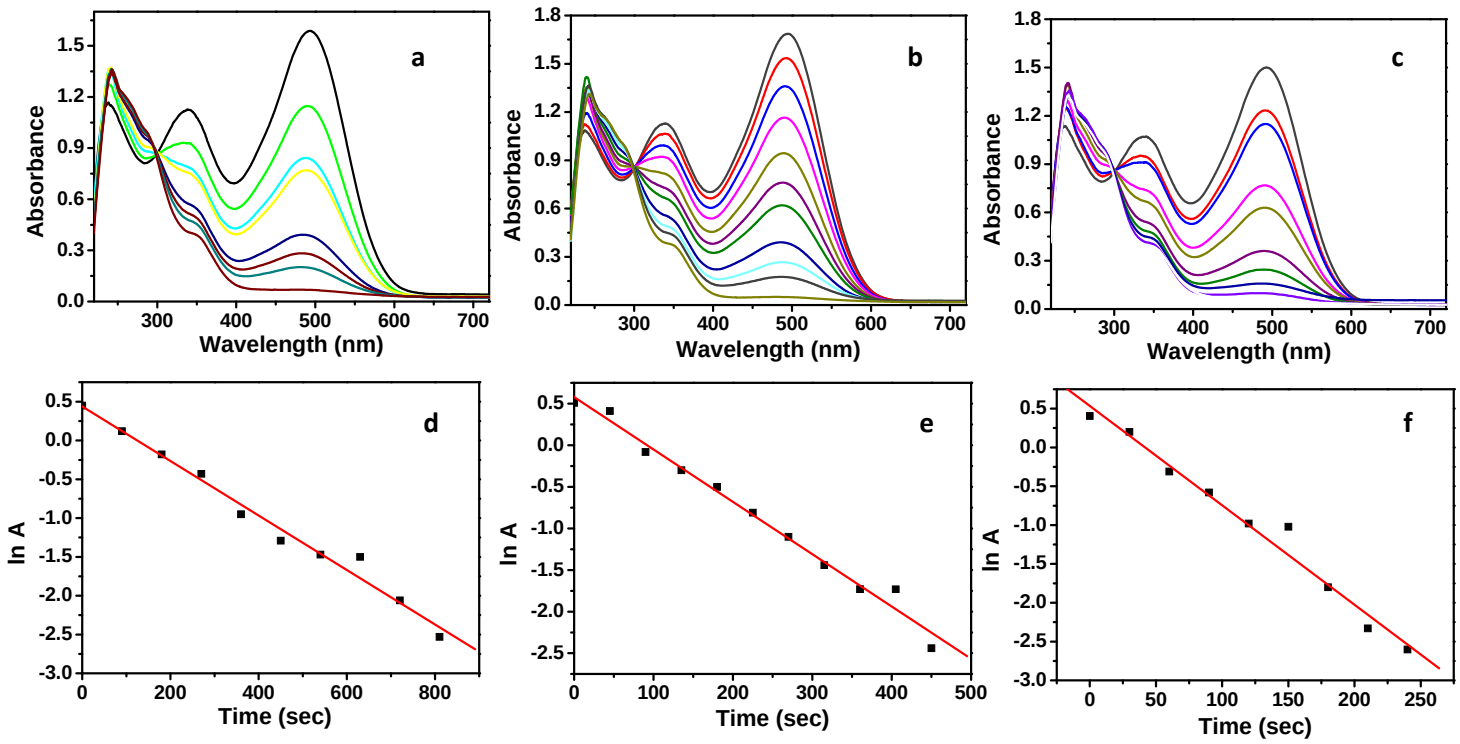


**Fig. S8** UV-Vis kinetic spectra for the degradation of congo red measured in varies time intervals using (a, b, c) AuNPs/GO-G1,2,3PAMAM dendrimer respectively. ln A vs Time plot for degradation of congo red by (d, e, f) AuNPs/GO-G1,2,3PAMAM dendrimer respectivley.

### 3. Effect of catalytic dosage

The effect of amount of catalyst on the rate of the reaction was determined by varying the catalytic dosage with respect to the identical concentration of $NaBH_4$ and azo dyes.

**Catalytic dosage of AgNPs/GO-G3PAMAM in degradation of Methyl orange**

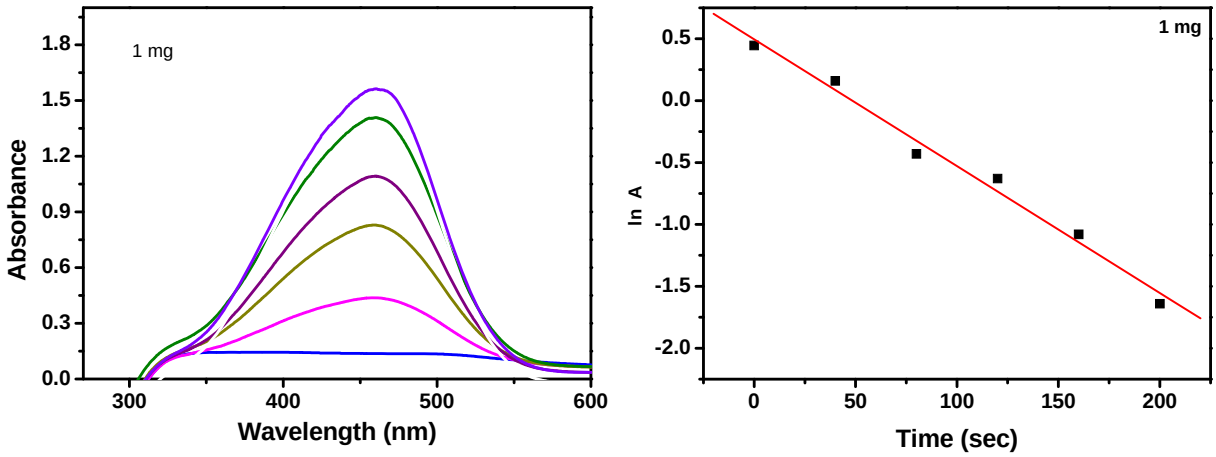


**Fig. S9.** UV-Visible kinetics spectrum for the degradation of methyl orange using 1 mg (AgNPs/GO-G3PAMAM). The obtained rate constant is (k) 10.2 x $10^{-3}$ $s^{-1}$

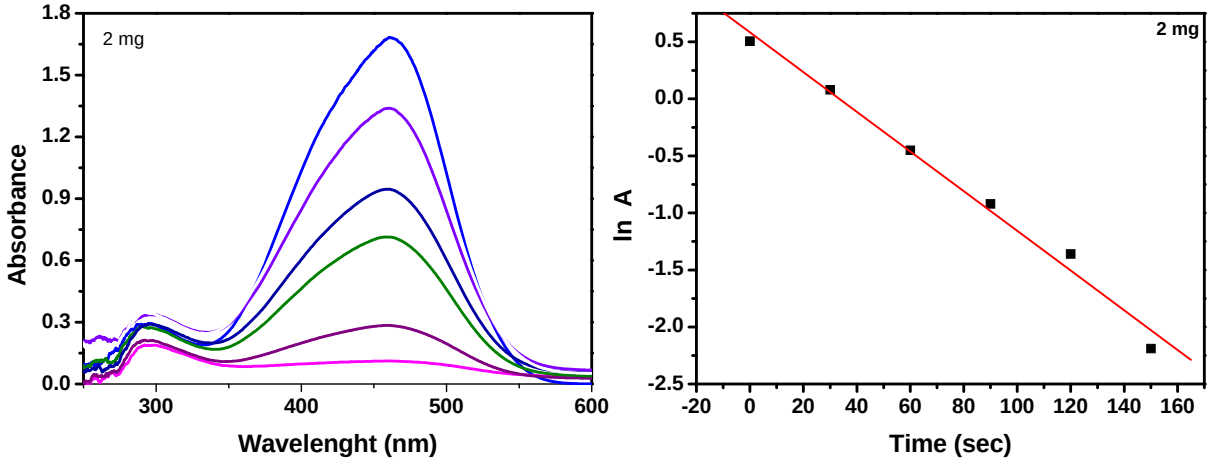


**Fig. S10.** UV-Visible kinetics spectrum for the degradation of methyl orange using 2 mg (AgNPs/GO-G3PAMAM). The obtained rate constant is (k) 17.4 x $10^{-3}$ $s^{-1}$

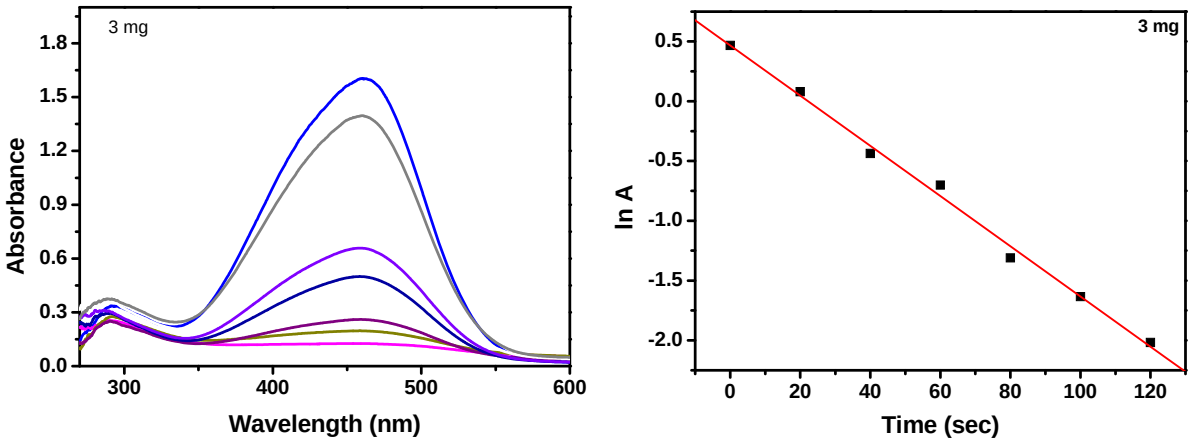


**Fig. S11**. UV-Visible kinetics spectrum for the degradation of methyl orange using 3 mg (AgNPs/GO-G3PAMAM). The obtained rate constant is (k) 20.9 x $10^{-3}$ $s^{-1}$

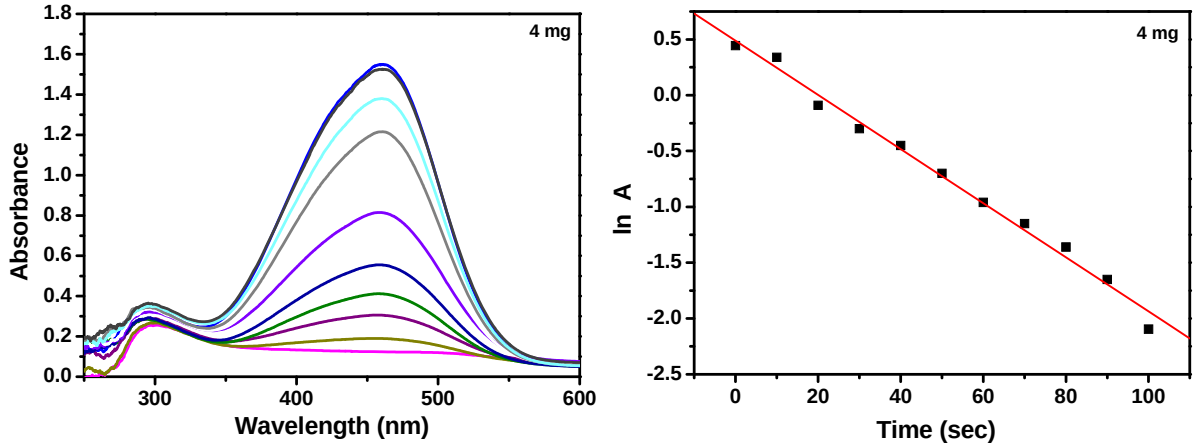


**Fig. S12.** UV-Visible kinetics spectrum for the degradation of methyl orange using 4 mg (AgNPs/GO-G3PAMAM). The obtained rate constant is (k) 24.2 x $10^{-3}$ $s^{-1}$

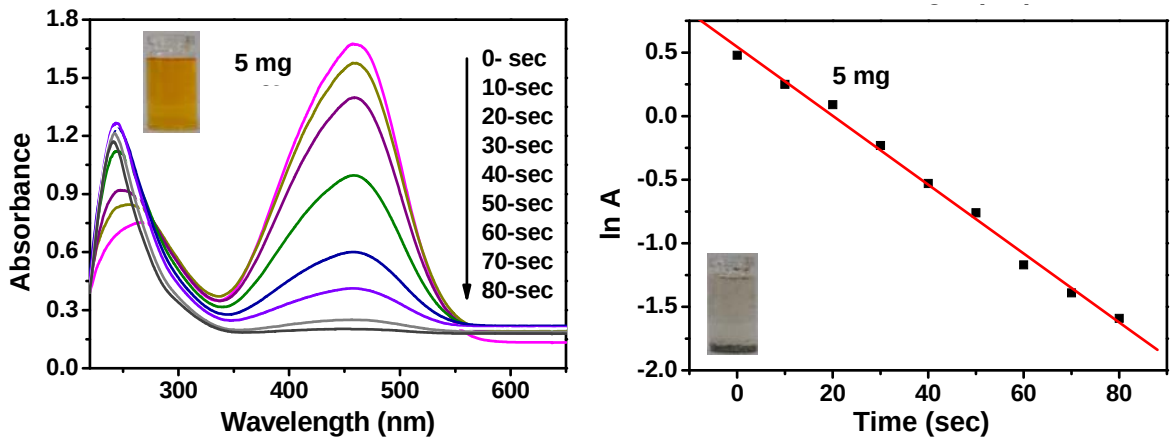


**Fig. S13.** UV-Visible kinetics spectrum for the degradation of methyl orange using 5 mg (AgNPs/GO-G3PAMAM). The obtained rate constant is (k) 25.9 x $10^{-3}$ $s^{-1}$

**Catalytic dosage of AgNPs/GO-G3PAMAM in degradation of Congo red**

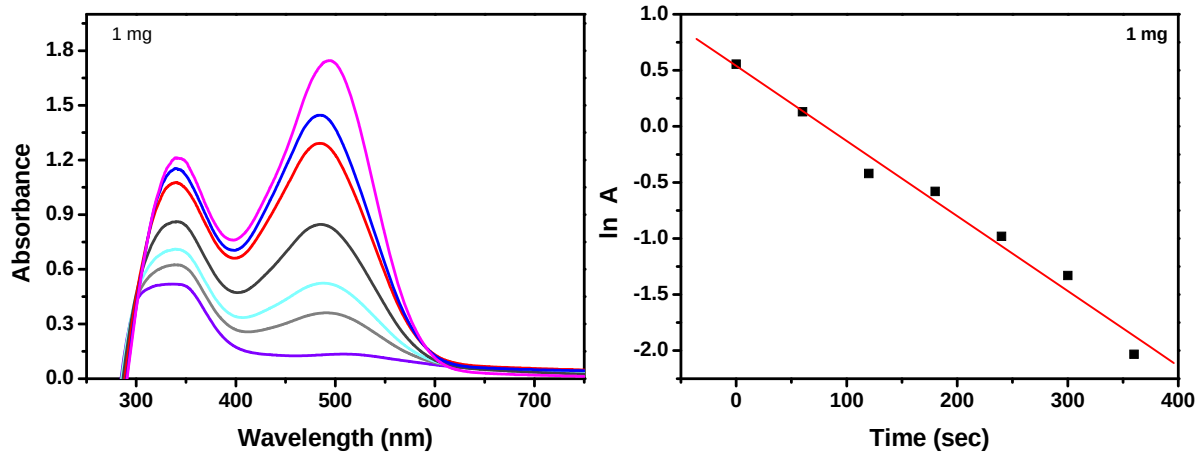


**Fig. S14.** UV-Visible kinetics spectrum for the degradation of congo red using 1 mg (AgNPs/GO-G3PAMAM). The obtained rate constant is (k) 5.88 x $10^{-3}$ $s^{-1}$

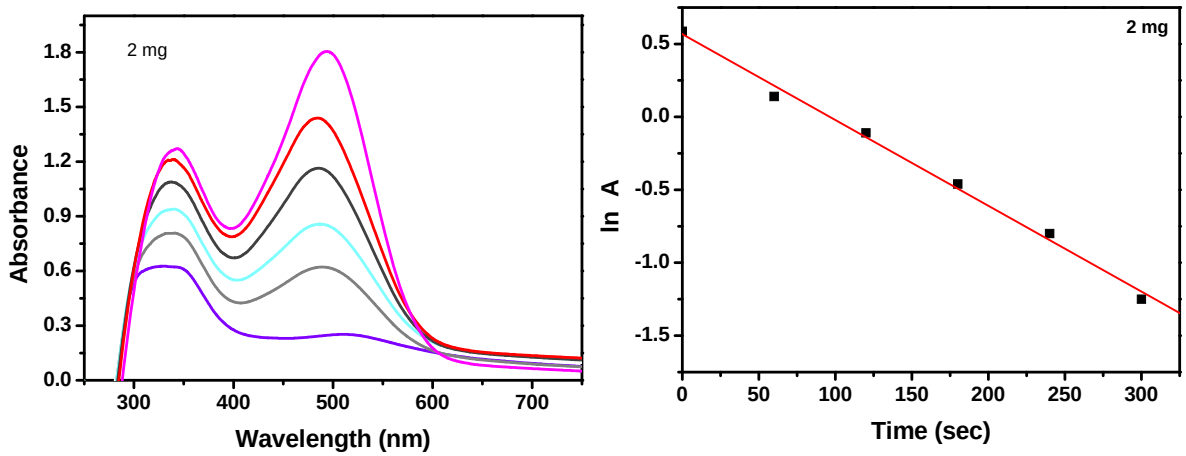


**Fig. S15.** UV-Visible kinetics spectrum for the degradation of congo red using 2 mg (AgNPs/GO-G3PAMAM). The obtained rate constant is (k) 6.69 x $10^{-3}$ $s^{-1}$

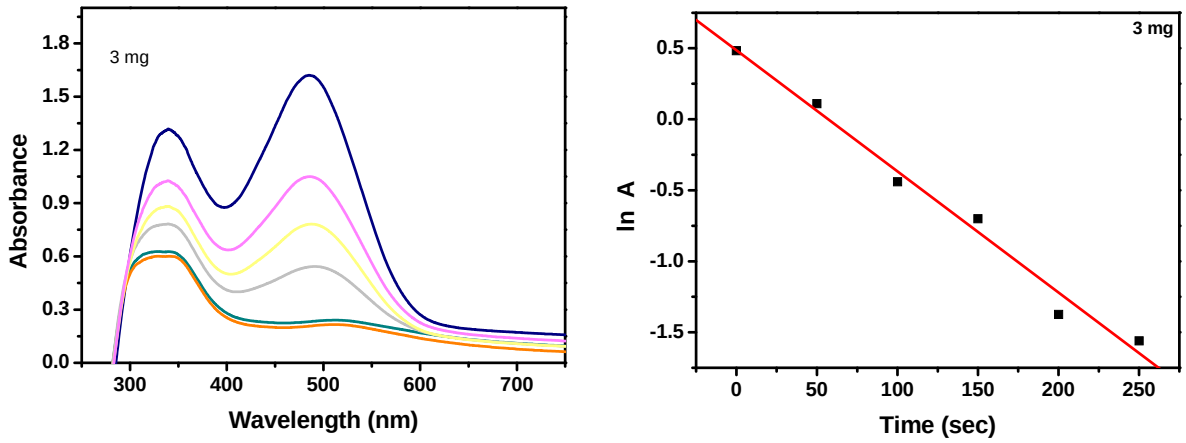


**Fig. S16.** UV-Visible kinetics spectrum for the degradation of congo red using 3 mg (AgNPs/GO-G3PAMAM). The obtained rate constant is (k) 8.53 x $10^{-3}$ $s^{-1}$

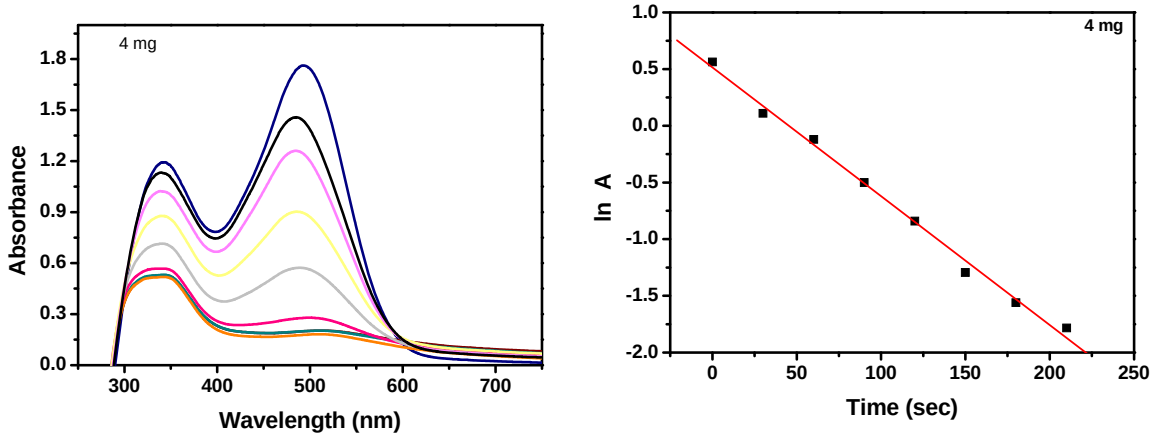


**Fig. S17.** UV-Visible kinetics spectrum for the degradation of congo red using 4 mg (AgNPs/GO-G3PAMAM). The obtained rate constant is (k) 11.37 x $10^{-3}$ $s^{-1}$

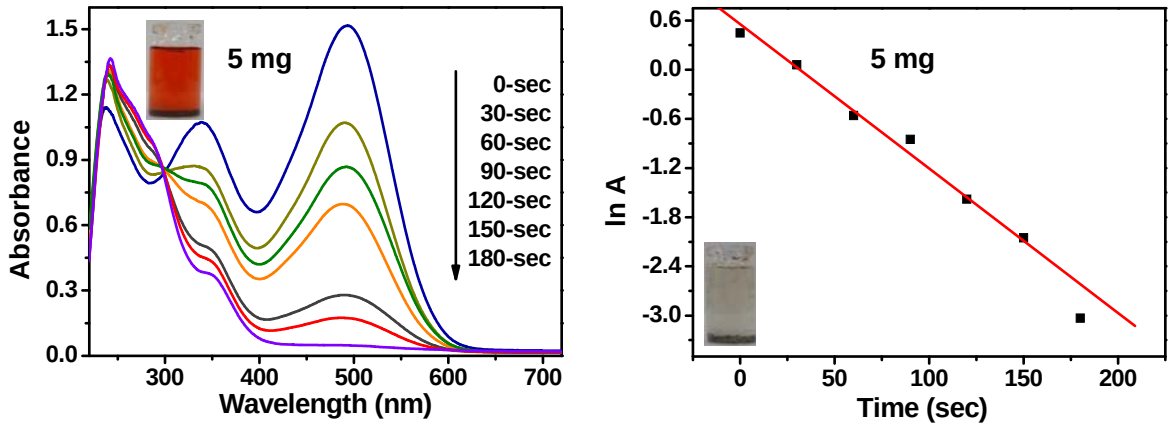


**Fig. S18.** UV-Visible kinetics spectrum for the degradation of congo red using 5 mg (AgNPs/GO-G3PAMAM). The obtained rate constant is (k) 19.1 x $10^{-3}$ $s^{-1}$

Similarly, we measured degradations rate constants for methyl orange and congo red dyes using different amount of nano catalyst (1 to 5 mg) with all generation PAMAM dendrimer grafted GO stabilised Ag and AuNPs. The obtained rate constants plotted against with different amount of catalysts.

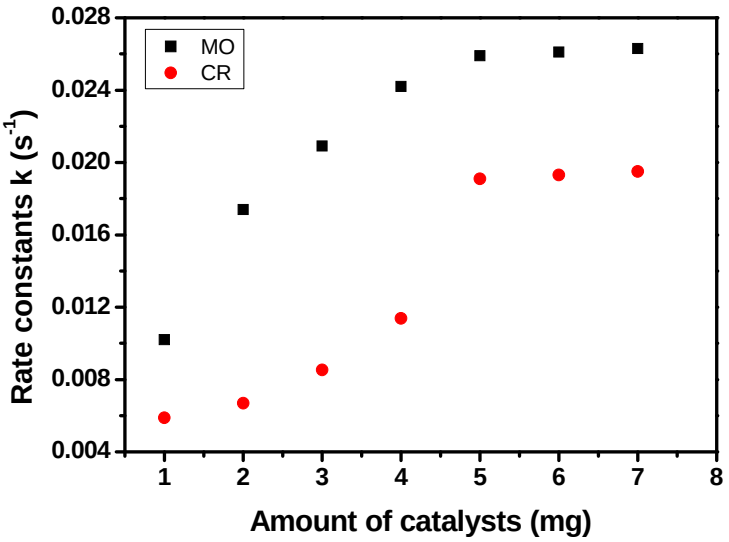


**Fig. S19.** Catalytic dosage for degradation of Methyl orange and Congo red was carried out at room temperature using different amount of AgNPs-GO-G3PAMAM.

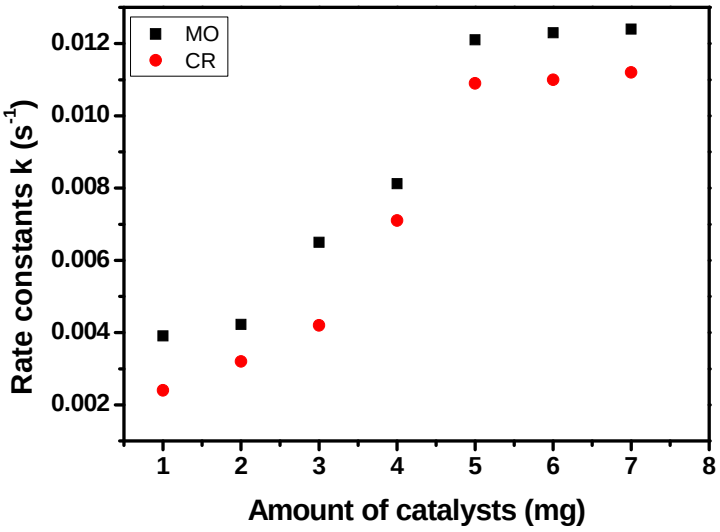


**Fig. S20.** Catalytic dosage for degradation of Methyl orange and Congo red was carried out at room using different amount of AgNPs-GO-G2PAMAM.

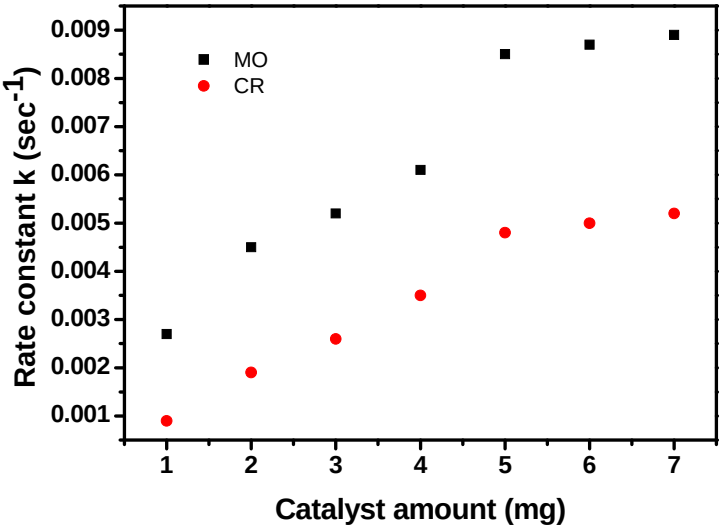


**Fig. S21.** Catalytic dosage for degradation of Methyl orange and Congo red was carried out at room using different amount of AgNPs-GO-G1PAMAM.

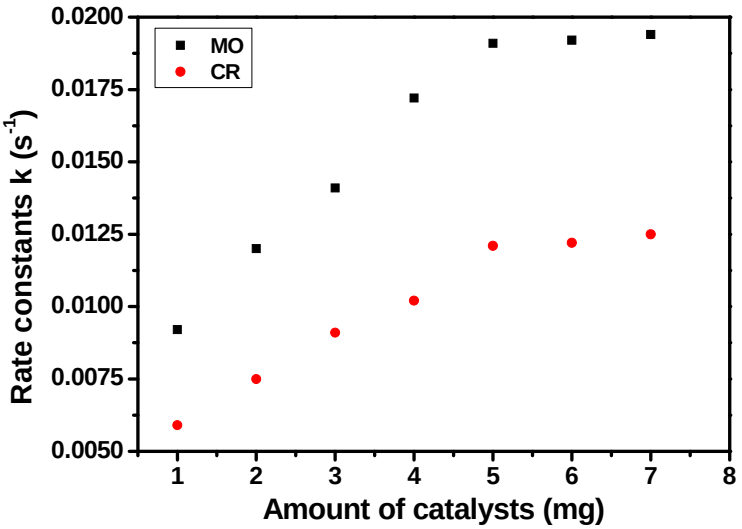


**Fig. S22.** Catalytic dosage for degradation of Methyl orange and Congo red was carried out at room temperature using different amount of AuNPs-GO-G3PAMAM.

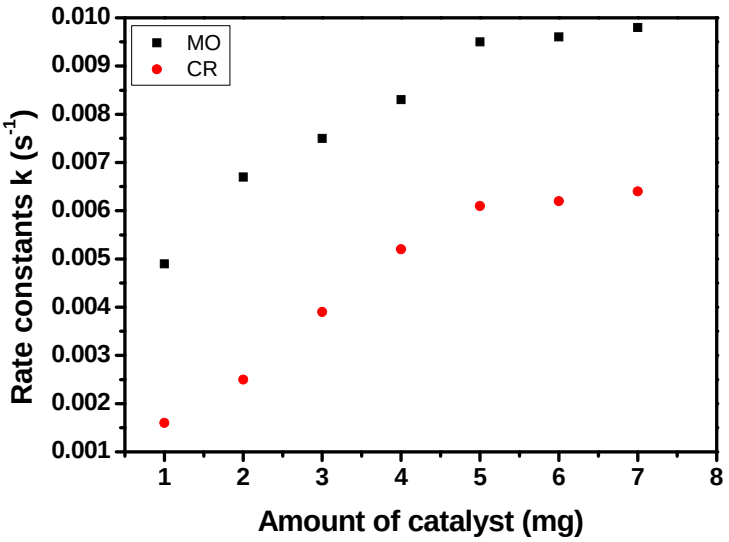


**Fig. S23.** Catalytic dosage for degradation of Methyl orange and Congo red was carried out at room temperature using different amount of AuNPs-GO-G2PAMAM.

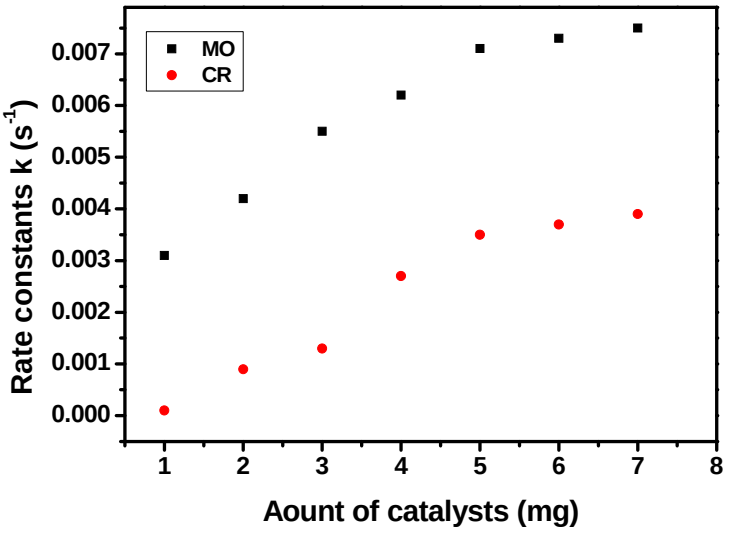


**Fig. S24.** Catalytic dosage for degradation of Methyl orange and Congo red was carried out at room temperature using different amount of AuNPs-GO-G1PAMAM.

It can be seen from Fig. S9-24, it was found that, with an increase the amount of catalysts the rate of the degradation is increases.

**4. Reusability of the catalysts**

Stability and recyclability is importance for the practical applications of catalysts. After the degradations the catalyst was easily recovered by centrifugation and washed three times with distilled water. Centrifugal separation provides a very convenient approach for removing and recycling by applying centrifugal force. The reusability of the catalysts was studied **(Fig. S25)**, after the first cycle and then which was recycled for 10 successive cycles without significant loss of its activity.

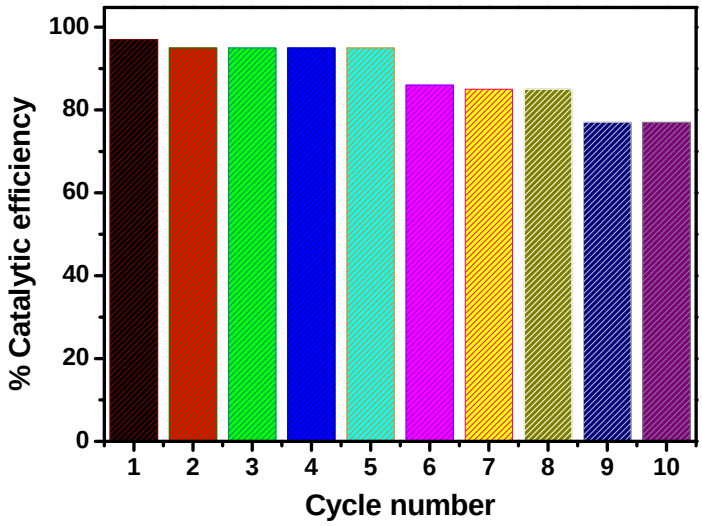


**Fig. S25.** Degradation of methyl orange using AgNPs-GO-G3PAMAM over ten successive reuse cycles. Conditions: MO = 1 x$10^{-6}$ M; amount of AgNPs-GO-G3PAMAM catalyst = 5 mg; [$NaBH_4$] = 50 µL (0.1 M) $NaBH_4$ in 3 mL.

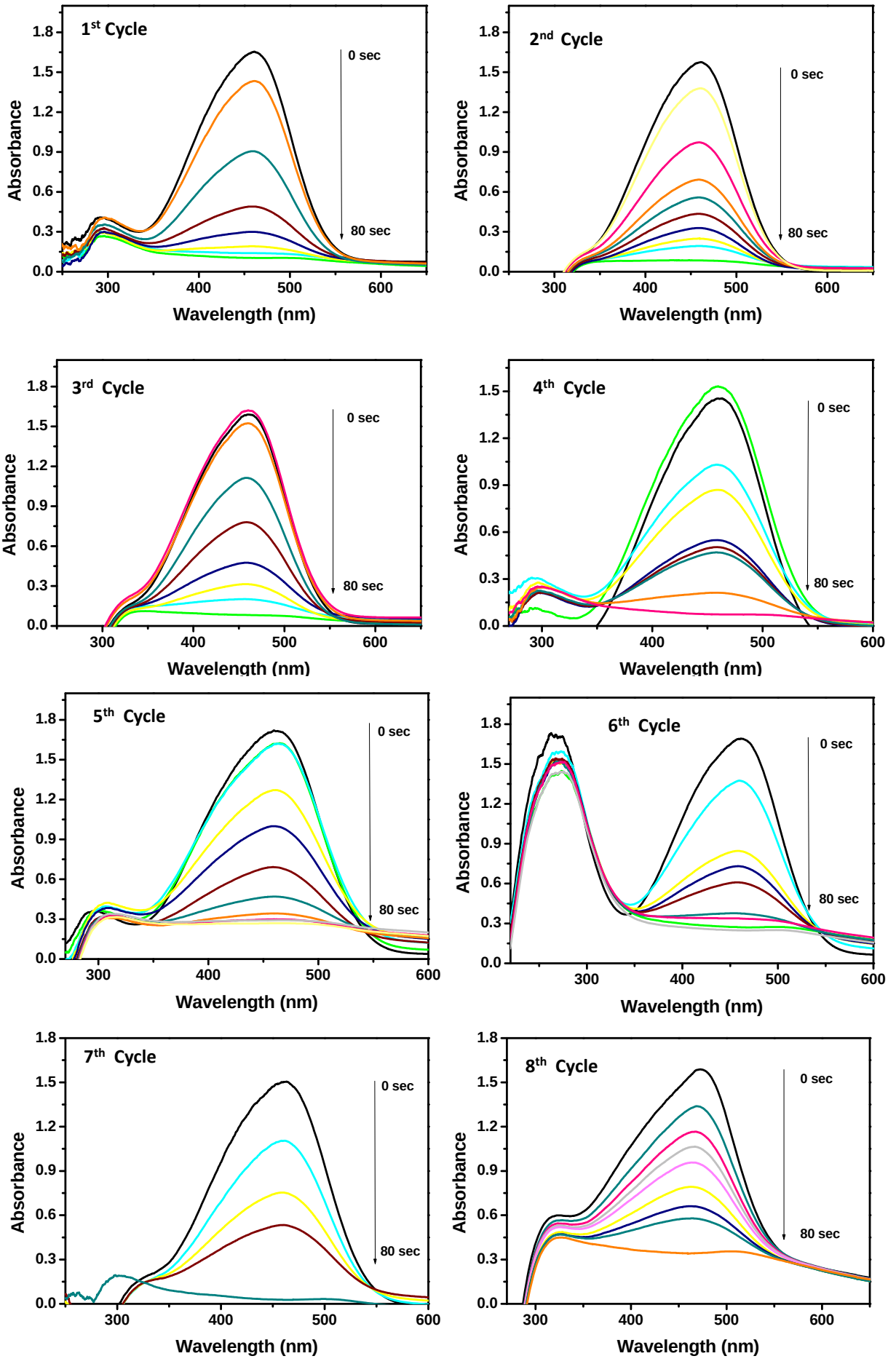

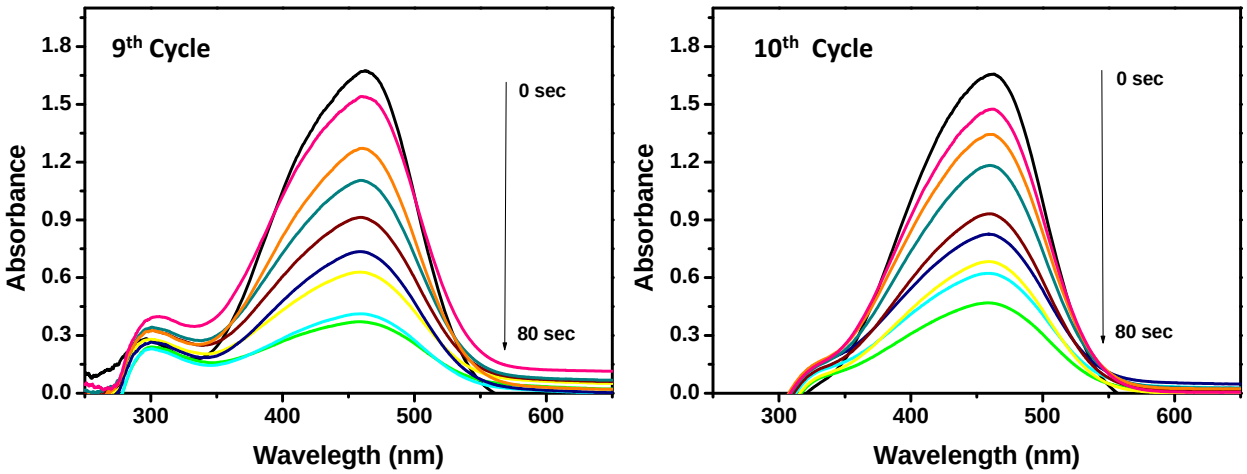


**Fig. S26.** UV-Visible kinetic spectrum for degradation of methyl orange using AgNPs-GO-G3PAMAM over ten successive reuse cycles. Conditions: MO = 1 x$10^{-6}$ M; amount of AgNPs-GO-G3PAMAM catalyst = 5 mg; [$NaBH_4$] = 50 µL (0.1 M) $NaBH_4$ in 3 mL.

**Fig. S26** shows 1 to 10 recycles for UV-Visible kinetic degradation spectrum of methyl orange azo dye by AgNPs-GO-G3PAMAM, it can be seen after 10 successive cycles there is no significant loss of its activity.

## 5. Characterisation of degraded organic compounds

### 5.1 FT-IR Spectroscopy studies of degraded organic compounds

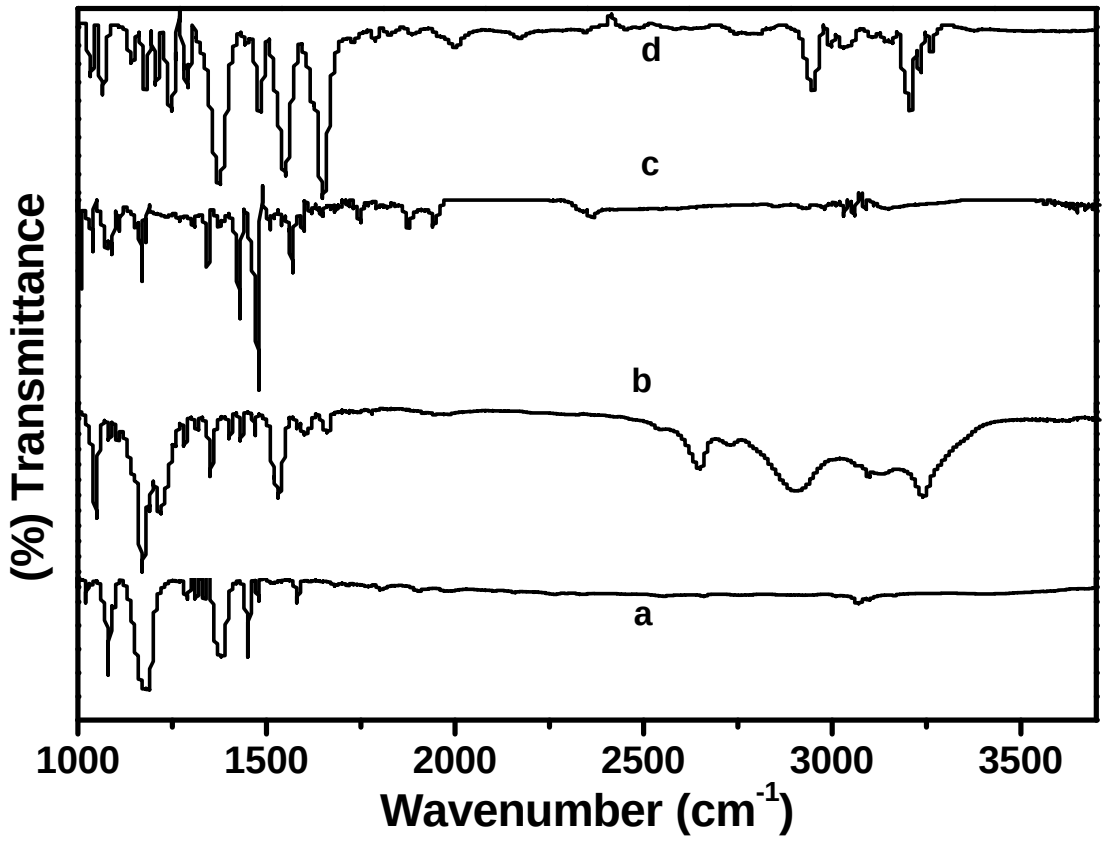


**Fig. S27.** FT-IR Spectra for the degraded organic compounds namely (a) Benzenesulfonic acid sodium salt, (b) 4-amino-1-naphthalenesulfonic acid sodium salt, (c) Biphenyl and (d) N,N'-Dimethyl aniline.

After the dye degradations the organic compounds was extracted with solvents and are characterized with FT-IR spectroscopy. The extracted Benzenesulfonic acid sodium salt (Fig. S27 (a) was confirmed through the appearance of aromatic -C=C- peak at 1581 $cm^{-1}$ and sulfonate ($-SO_3^-$ $Na^+$) peak at 1030 $cm^{-1}$. In the case of 4-amino-1-naphthalenesulfonic acid sodium salt (Fig. S27 b) exist broad and intense peaks at 1172 and 1079 $cm^{-1}$ due to ($-SO_3^-$ $Na^+$) group and also new peaks are appeared at 1581 $cm^{-1}$ and 3220 $cm^{-1}$ for characteristic stretching vibrations of -C=C- and $-NH_2$ groups respectively. In Fig. S27 (c) FT-IR spectrum of Biphenyl shows a new peaks appeared at 3010 $cm^{-1}$ and 1605 $cm^{-1}$ due to the aromatic –

CH and -C=C- functional groups respectively. In Fig. S27 (d) the observed multiple bands around 3042 $cm^{-1}$ is assigned to the aromatic -CH and aliphatic -$CH_3$ stretching modes. Other peaks at 2812 represents to vibrations stretching frequency of [C–H of $N(CH_3)_2$] groups indicates the formations of the N,N'-Dimethyl aniline organic compound.

### 5.2 $^1$H-NMR Spectroscopy of degraded organic compounds

After the dye degradations the organic compounds was extracted with solvents and are characterized with $^1$H-NMR spectroscopy.

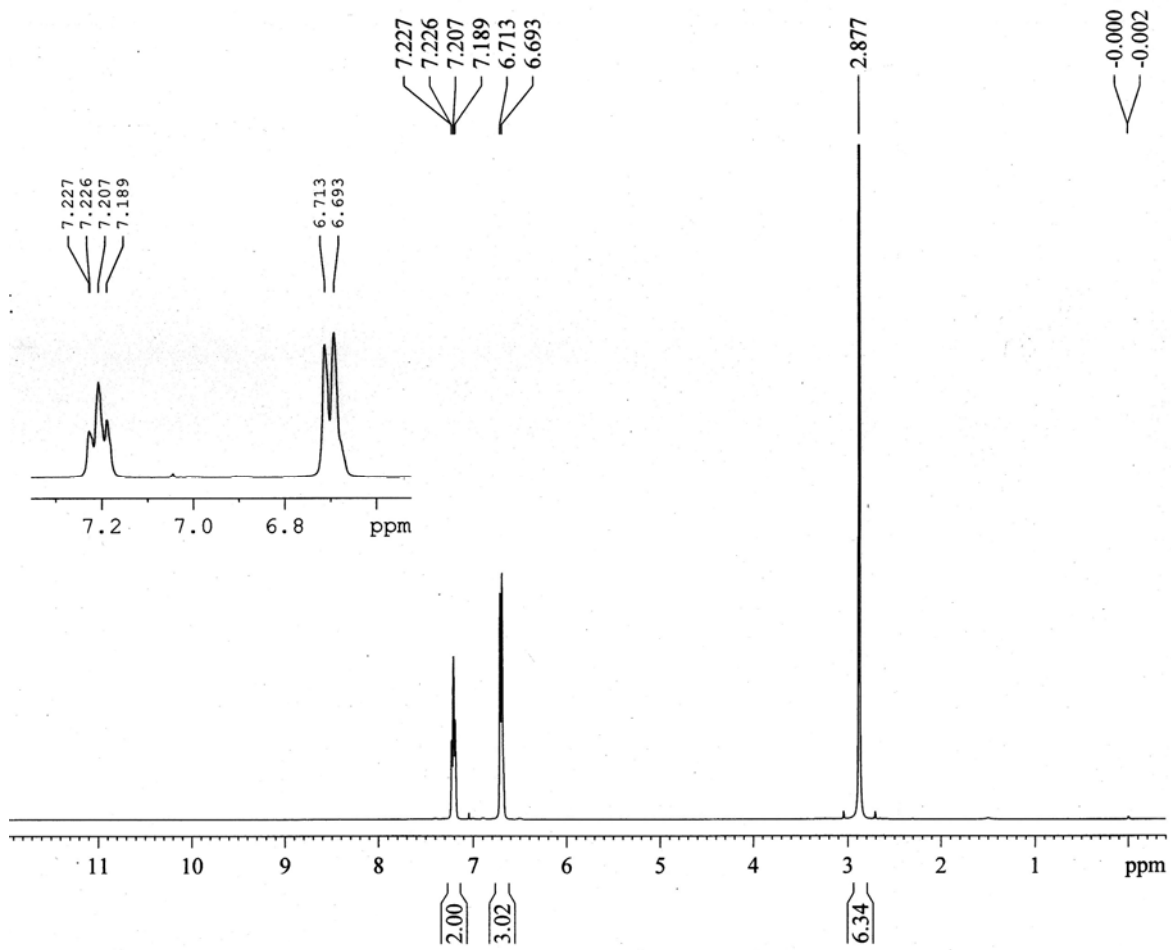


**Fig. S28** $^1$H-NMR of N,N'-Dimethyl aniline

**N,N'-Dimethyl aniline:** $^1$H-NMR (400 MHz, $CDCl_3$) δ 7.21 (m, 2H), δ 6.71 (d, 3H), δ 2.87 (s, 6H).

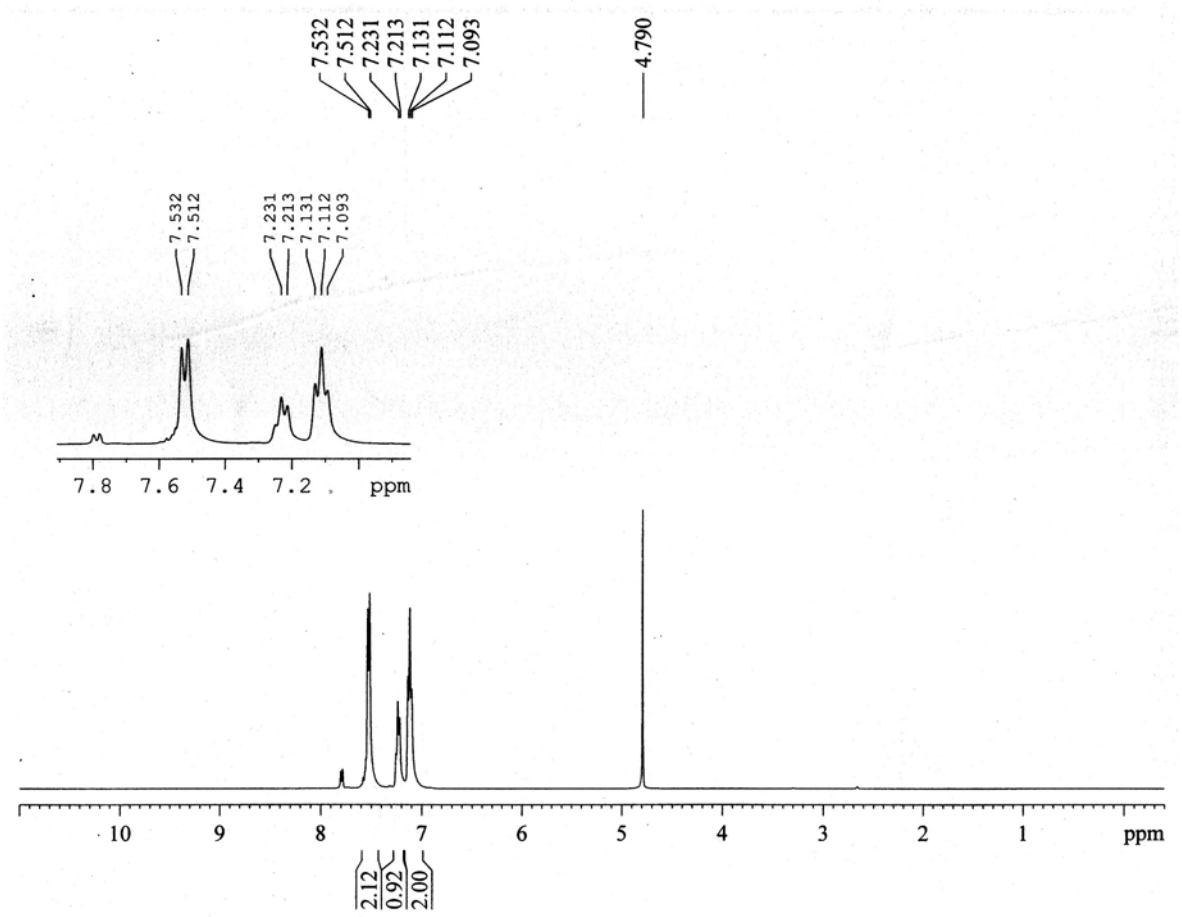


**Fig. S29** $^{1}$H-NMR of Benzenesulfonic acid sodium salt

**Benzenesulfonic acid sodium salt:** $^{1}$H-NMR (400 MHz, $D_2O$) δ 7.53 (d, 2H), δ 7.23 (d, 1H), δ 7.13 (t, 2H).

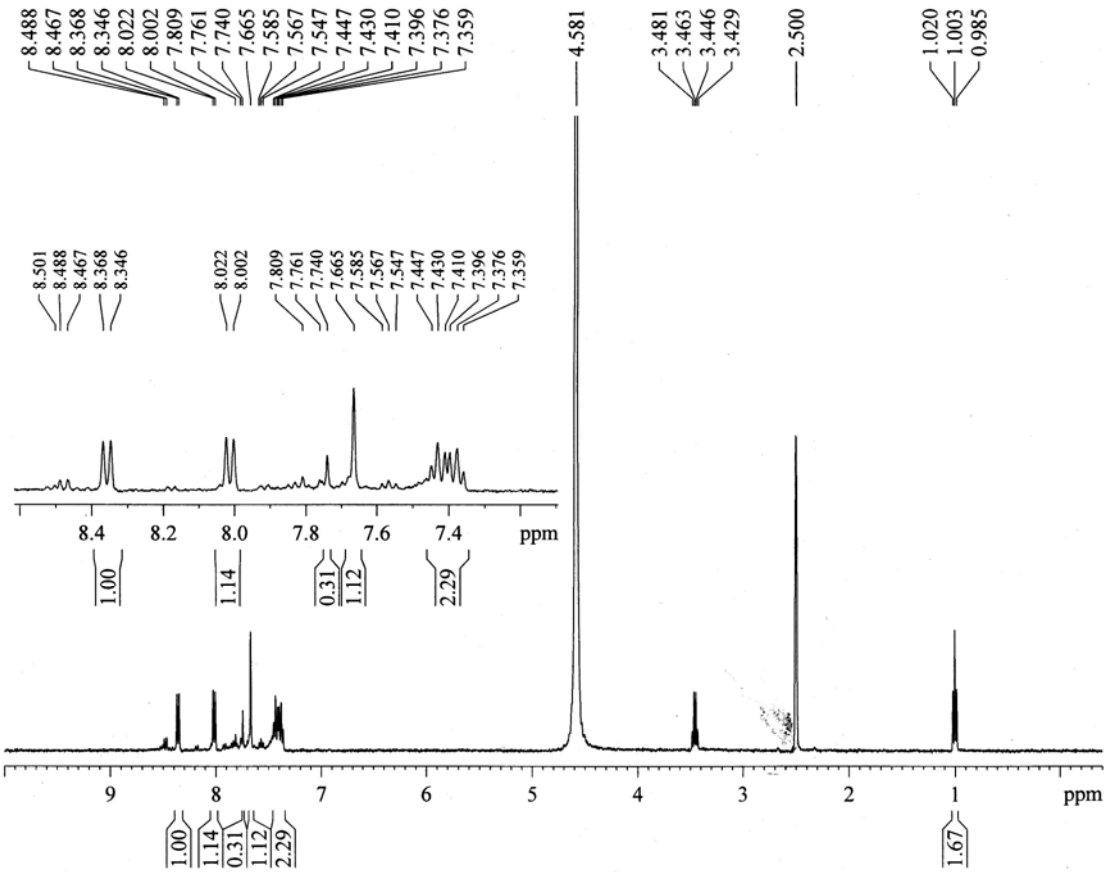


**Fig. S30** $^{1}$H-NMR of 4-Amino-1-naphthalenesulfonic acid sodium salt

**4-Amino-1-naphthalenesulfonic acid sodium salt:** $^{1}$H-NMR (400 MHz, $D_2O$ + 1 drop DDMSO) δ 8.36 (d, 1H), δ 8.02 (d, 1H), δ 7.66 (s, 2H), δ 7.43 (m, 4H).

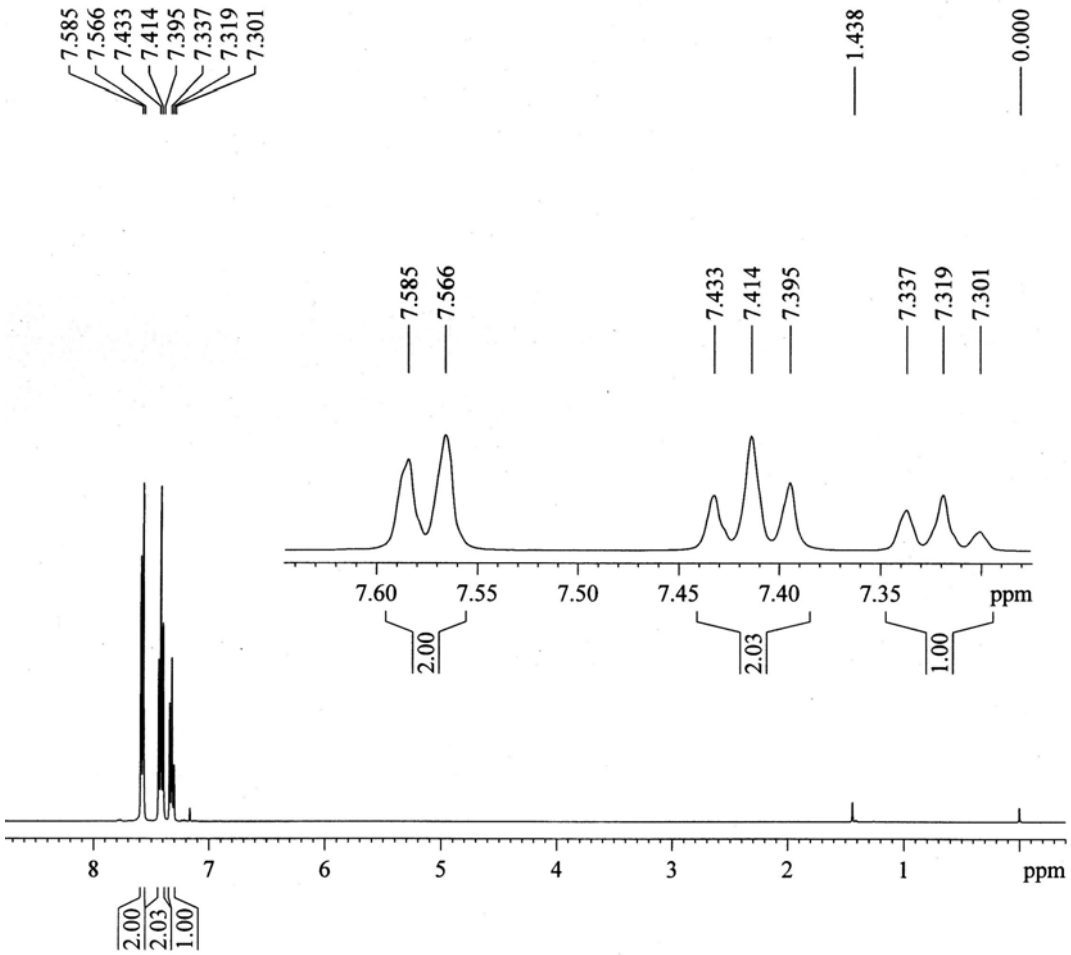


**Fig. S31** $^{1}$H-NMR of Biphenyl

**Biphenyl:** $^{1}$H-NMR (400 MHz, $CDCl_3$) δ 7.57 (d, 2H), δ 7.43 (t, 2H), δ 7.33 (t, 1H)

**Table S1:** Parameters of $N_2$ adsorption isotherm measurement

| **Samples**[a] | **Surface area ($m^2$ $g^{-1}$)**[b] |
|---|---|
| GR[c] | 8.7 |
| GO[d] | 185 |
| AgNPs-GO-G1PAMAM[e] | 290 |
| AgNPs-GO-G2PAMAM[e] | 330 |
| AgNPs-GO-G3PAMAM[e] | 365 |
| AuNPs-GO-G1PAMAM[f] | 293 |
| AuNPs-GO-G2PAMAM[f] | 325 |
| AuNPs-GO-G3PAMAM[f] | 358 |

[a]50 mg of sample have been used for recording BET isotherm, [b]BET specific surface area was calculated from the linear part of the corresponding BET plot, [c]Pure graphite, [d]Graphene oxide, [e]GO grafted first, second and third generation PAMAM dendrimer encapsulated AgNPs, [f]GO grafted first, second and third generation PAMAM dendrimer encapsulated AuNPs,

## 6. References

[1] W. Yuan, G. Jiang, J. Che, X. Qi, R. Xu, W. Matthew, Chang, Y. Chen, S. Yin Lim, J. Dai, B. Mary, C. Park, *J. Phys. Chem. C,* 2008, **112,** 18754.

[2] Xing Lu, Toyoko Imae, *J. Phys. Chem. C,* 2007, **111,** 2416.

[3] S. Zhen Zu, B. Hang Han, *J. Phys. Chem. C,* 2009, **113,** 13651.

[4] S. Wakelanda, R. Martineza, K. John, Greyb, C. Claudia, Luhrsa, *Carbon,* 2010, **48(12)**, 3463.

[5] X. Tang, W. Li, Z. Yu, A. Mohammad, Rafiee, J. Rafiee, F. Yavari, N. Koratkar, *Carbon,* 2011, **49,** 1258.

[6] S. Stankovich, A. Dmitriy. Dikin, D. Richard, Piner, A. Kevin, Kohlhaas, A. Kleinhammes, Y. Jia, Y. Wu, T. SonBinh, Nguyen, S. Rodney, Ruoff. *Carbon,* 2007, **45,** 1558.

[7] Y. Yang, C. Pong Tsui, C. Yin Tang, S. Qiu, Q. Zhao, X. Cheng, Z. Sun, R. Kwok Yiu Li, X. Xie, *Eur. Polym. J.,* 2010, **46,** 145.

[8] Y. Guo, C. Bao, L. Song, B. Yuan, and Y. Hu, *Ind. Eng. Chem. Res.,* 2011, **18.**

[9] J. Shen, Y. Hu, M. Shi, N. Li, H. Ma, and M. Ye, *J. Phys. Chem. C,* 2010, **114,** 1498.